

Andrzej Czarski, Piotr Matusiewicz

Computer simulation of lamellar microstructure

Komputerowa symulacja struktury płytkowej

Abstract

Other than granular and dispersive microstructures, the lamellar microstructure is one of the most-frequently observed traits in the case of metal alloys. This work defines a geometrical model of a lamellar microstructure and presents its stereological relationships as well as our computer-simulation results for this model. The applied methodology creates – at least from a theoretical point of view – a series of interesting possibilities in the field of quantitative description of this type of microstructure and examinations of the properties of the parameter estimators that quantitatively characterize it.

Keywords: lamellar microstructure, pearlite, interlamellar spacing

Streszczenie

Mikrostruktura płytkowa to – obok ziarnistej i dyspersyjnej – jedna z najczęściej spotykanych w przypadku stopów metali. W pracy zdefiniowano geometryczny model mikrostruktury płytkowej, przedstawiono dla tego modelu zależności stereologiczne oraz wyniki symulacji komputerowej. Wykorzystana metodologia stwarza – przynajmniej z teoretycznego punktu widzenia – szereg nowych interesujących możliwości w zakresie ilościowego opisu tego typu mikrostruktur i badania własności estymatorów parametrów, które ją ilościowo charakteryzują.

Słowa kluczowe: struktura płytkowa, perlit

1. Introduction

The most-commonly known lamellar microstructure is pearlite – product from the eutectoid reaction in an Fe-Fe₃C system. The growth interaction between ferrite and cementite forms a microstructure with a lamellar morphology [1–3]. The lamellar morphology of parallel ferrite and cementite platelets in large colonies is dominating (Fig. 1). Local

Andrzej Czarski Ph.D. Eng., Piotr Matusiewicz Ph.D. Eng.: AGH University of Science and Technology, Faculty of Metals Engineering and Industrial Computer Science, Krakow, Poland; czarski@agh.edu.pl, matus@agh.edu.pl

deviations such as fiber-shaped cementites, rapid changes in platelet growth direction, disturbances in the vicinity of non-metallic inclusion, etc. are considered as a growth of structural errors [4–7].

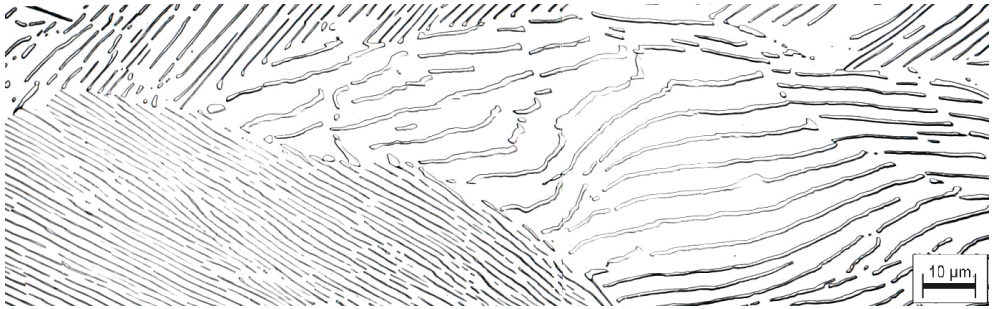


Fig. 1. Microstructure with coarse lamellar pearlite (etched in picral)

The quantitative parameters characterizing the lamellar microstructure [that is, true (l_t), apparent (l_a), and random (l_r) interlamellar spacing] have been defined by DeHoff, Rhines [8], and Underwood [9]. An estimation of l_a and l_r featuring our computer image analysis methods is presented in [10].

Determining the stereological relationships for this type of microstructure requires certain geometrical assumptions. The work of Czarski and Ryś [11, 12], which presents the basic stereological relations for lamellar microstructures, discusses the made assumptions for certain strictly defined geometrical model. Taking only into account the concept of interlamellar spacing, we can present this model as a packet of parallel planes; the spacing between the neighboring planes is a random variable, which is fully described by the function of density $f(l_r)$ (Fig. 2).

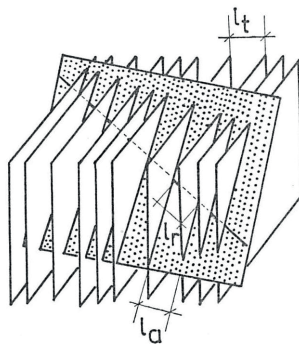


Fig. 2. Model of lamellar structure

2. Selected stereological relationships

On the basis of the defined geometrical model of the lamellar microstructure [11–15], we determined the relationships between the density function of true interlamellar spacing $f(l_t)$ and the density functions of random or apparent interlamellar spacing, $f(l_r)$ and $f(l_a)$, respectively. From a practical point of view, the relationships between function $f(l_t)$ and the density functions of the reciprocal of interlamellar spacings $f(l_r^{-1})$ and $f(l_a^{-1})$ will also be interesting.

The conditional density functions of random interlamellar spacing and the reciprocal of random interlamellar spacing [$f(l_r | l_t)$ and $f(l_r^{-1} | l_t)$, respectively] are presented below as well as apparent interlamellar spacing and the reciprocal of apparent interlamellar spacing ($f(l_a | l_t)$ and $f(l_a^{-1} | l_t)$, respectively) [11]:

$$f(l_r | l_t) = l_t / l_r^2; \quad l_t \leq l_r < \infty \quad (1)$$

$$f(l_r^{-1} | l_t) = l_t; \quad 0 < l_r^{-1} \leq l_t^{-1} \quad (2)$$

$$f(l_a | l_t) = \frac{l_t^2}{l_a^2 \sqrt{l_a^2 - l_t^2}}; \quad l_t \leq l_a < \infty \quad (3)$$

$$f(l_a^{-1} | l_t) = \frac{l_t^2}{\sqrt{l_a^2 - l_t^2}}; \quad 0 < l_a^{-1} \leq l_t^{-1} \quad (4)$$

Obviously, the density functions of random and apparent interlamellar spacing [$f(l_r)$ and $f(l_a)$, respectively] constitute the solution of the integral equations:

$$f(l_r) = \int_0^{l_r} f(l_r | l_t) f(l_t) dl_t \quad (5)$$

$$f(l_a) = \int_0^{l_a} f(l_a | l_t) f(l_t) dl_t \quad (6)$$

3. Computer model simulation

The simulation of the discussed model was performed in the following way:

1. l_t is a random number generated from the distribution described by function $f(l_t)$; l_t is the spacing between the determined planes $z = 0$ and $z + l_t = 0$
2. Generation of random vector $\bar{r} = [a, b, c]$ describing straight line $\frac{x}{a} + \frac{y}{b} + \frac{z}{c}$ and plane $ax + by + cz = 0$, which cross parallel planes $z = 0$ and $z + l_t = 0$
3. Calculation of the values of $l_r, l_r^{-1}, l_a, l_a^{-1}$

The random number generators from the CERN Program Library were used.

The testing range of the applied generators included the Pearson chi-square test, the Wald–Wolfowitz runs test, and (within the frames of the so-called combinatory tests) the poker test [16–19].

The calculations were performed in the Lahey/Fujitsu Fortran environment.

4. Simulation results

Three cases will be presented according to the assumed distribution of true interlamellar spacing (function $f(l_t)$). For each, the distributions of parameters $l_r, l_r^{-1}, l_a, l_a^{-1}$ were determined both analytically and as a result of the simulations.

True interlamellar spacing is constant ($l_t = \text{const}$)

Analytical solution. In this case, density functions $f(l_r), f(l_r^{-1}), f(l_a)$, and $f(l_a^{-1})$ correspond to density functions (1), (2), (3), and (4), respectively:

$$f(l_r) = l_t / l_r^2; \quad l_t \leq l_a < \infty \tag{7}$$

$$f(l_r^{-1}) = l_t; \quad 0 < l_r^{-1} \leq l_t^{-1} \tag{8}$$

$$f(l_a) = \frac{l_t^2}{l_a^2 \sqrt{l_a^2 - l_t^2}}; \quad l_t \leq l_a < \infty \tag{9}$$

$$f(l_a^{-1}) = \frac{l_t^2}{\sqrt{(l_a^{-1})^{-2} - l_t^2}}; \quad 0 < l_a^{-1} \leq l_t^{-1} \tag{10}$$

The simulation results are presented in Figures 3 and 4.

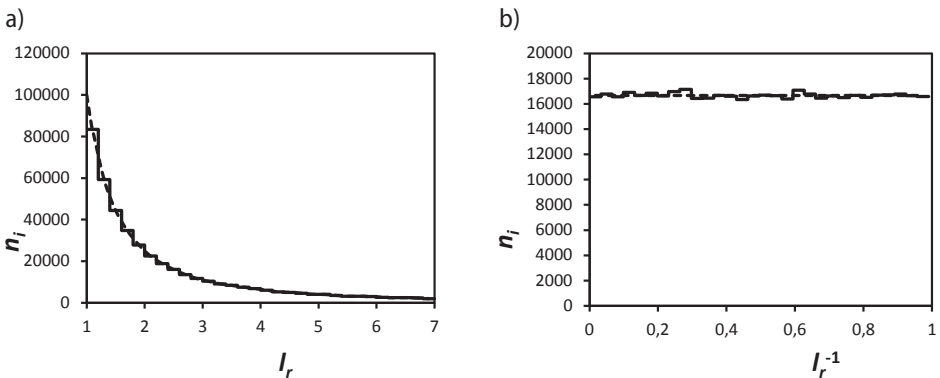


Fig. 3. Distribution of random interlamellar spacing l_r (a) and the reciprocal of random interlamellar spacing l_r^{-1} (b) with the assumption of constant true interlamellar spacing, $l_t = 1$

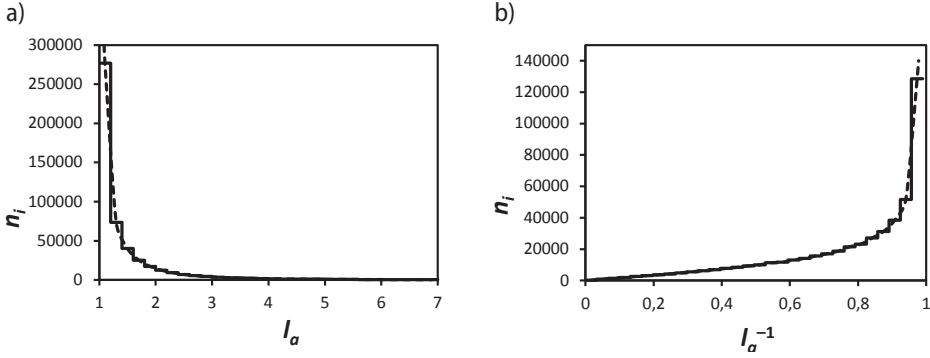


Fig. 4. Distribution of apparent interlamellar spacing l_a (a) and the reciprocal of apparent interlamellar spacing l_a^{-1} (b) with the assumption of constant true interlamellar spacing, $l_t = 1$

True interlamellar spacing has a uniform distribution

In the case of uniform distribution, the density function of true interlamellar spacing has the following form:

$$f(l_t) = \frac{1}{l_{t \max} - l_{t \min}}; \quad l_{t \min} < l_t < l_{t \max} \quad (11)$$

where: $l_{t \min}$, $l_{t \max}$ are the minimal and maximal values of true interlamellar spacing, respectively.

Analytical solutions:

$$f(l_r) = \begin{cases} \frac{1}{2(l_{t \max} - l_{t \min})} \left(1 - \frac{l_{t \min}^2}{l_r^2} \right); & l_{t \min} \leq l_r < l_{t \max} \\ \frac{1}{2l_r^2 (l_{t \max} - l_{t \min})}; & l_{t \max} \leq l_r < \infty \end{cases} \quad (12)$$

$$f(l_a) = \begin{cases} \frac{1}{2(l_{t \max} - l_{t \min})} \left(\frac{\pi}{2} - \arcsin \frac{l_{t \min}}{l_a} - \frac{l_{t \min}}{l_a^2} \sqrt{l_a^2 - l_{t \min}^2} \right) & l_{t \min} \leq l_a < l_{t \max} \\ \frac{1}{2l_a^2 (l_{t \max} - l_{t \min})} \left(l_{t \min} \sqrt{l_a^2 - l_{t \min}^2} - l_{t \max} \sqrt{l_a^2 - l_{t \max}^2} \right) + & l_{t \max} \leq l_a < \infty \\ \frac{1}{2(l_{t \max} - l_{t \min})} \left(\arcsin \frac{l_{t \max}}{l_a} - \arcsin \frac{l_{t \min}}{l_a} \right) & \end{cases} \quad (13)$$

$$f(l_r^{-1}) = \begin{cases} \frac{1}{2}(l_{t \max} + l_{t \min}); & 0 \leq l_r^{-1} < l_{t \max}^{-1} \\ \frac{1}{2(l_{t \max} + l_{t \min})} \left[(l_r^{-1})^{-2} - l_{t \min}^2 \right]; & l_{t \max}^{-1} \leq l_r^{-1} < l_{t \min}^{-1} \end{cases} \quad (14)$$

$$f(l_a^{-1}) = \begin{cases} \frac{1}{2l_a^{-1}(l_{t \max} - l_{t \min})} \left(l_{t \min} \sqrt{1 - l_{t \min}^2 (l_a^{-1})^2} - l_{t \max} \sqrt{1 - l_{t \max}^2 (l_a^{-1})^2} \right) + \\ \quad + \frac{1}{2(l_a^{-1})^2 (l_{t \max} - l_{t \min})} \times \\ \quad \times \arcsin \left(l_{t \max} l_a^{-1} \sqrt{1 - l_{t \min}^2 (l_a^{-1})^2} - l_{t \min} l_a^{-1} \sqrt{1 - l_{t \max}^2 (l_a^{-1})^2} \right) & 0 \leq l_a^{-1} < l_{t \max}^{-1} \\ \frac{1}{2(l_a^{-1})^2 (l_{t \max} - l_{t \min})} \left(l_{t \min} l_a^{-1} \sqrt{1 - l_{t \min}^2 (l_a^{-1})^2} - \right. \\ \quad \left. + \arcsin(l_{t \min} l_a^{-1}) + \frac{\pi}{2} \right); & l_{t \max}^{-1} \leq l_a^{-1} < l_{t \min}^{-1} \end{cases} \quad (15)$$

The results of the simulation are presented in Figures 5 and 6.

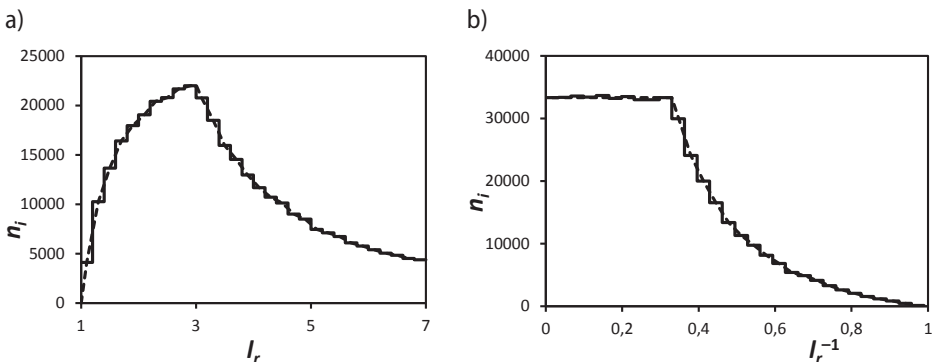


Fig. 5. Distribution of random interlamellar spacing l_r (a) and the reciprocal of random interlamellar spacing l_r^{-1} (b) with the assigned uniform distribution of true interlamellar spacing l_t obtained as a result of the simulation

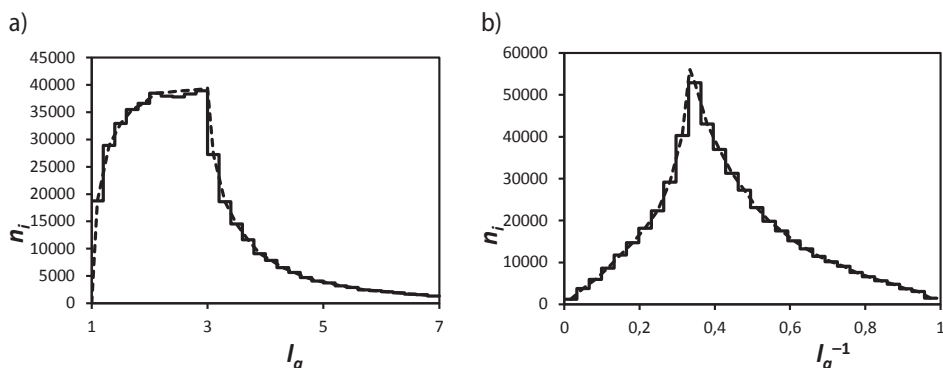


Fig. 6. Distribution of apparent interlamellar spacing l_a (a) and the reciprocal of apparent interlamellar spacing l_a^{-1} (b) with the assigned uniform distribution of true interlamellar spacing l_t obtained as a result of the simulation

True interlamellar spacing has a Rayleigh distribution

In the case of the Rayleigh distribution, the density function of true interlamellar spacing has the following form [16–17]:

$$f(l_t) = 2\lambda(l_t - l_{t\min})e^{-\lambda(l_t - l_{t\min})^2}; \quad l_{t\min} < l_t < \infty \quad (16)$$

where:

- $l_{t\min}$ – the minimal value of true interlamellar spacing,
- λ – distribution parameter.

The results of the simulation are presented in Figures 7 and 8.

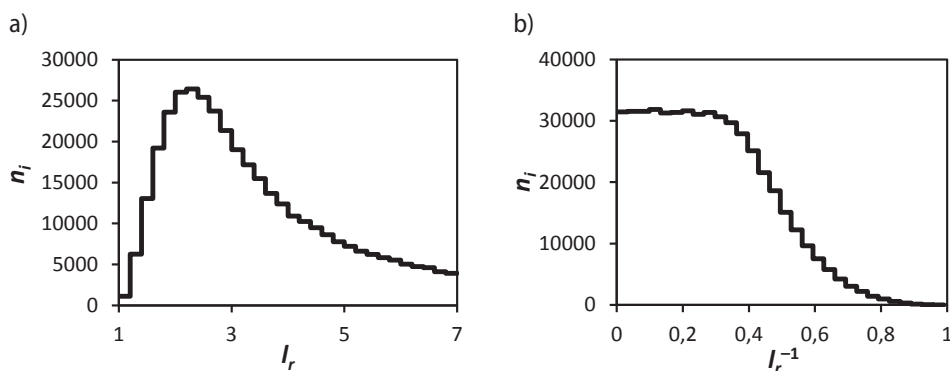


Fig. 7. Distribution of random interlamellar spacing l_r (a) and the reciprocal of random interlamellar spacing l_r^{-1} (b) with the assigned Rayleigh distribution of true interlamellar spacing l_t obtained as a result of the simulation

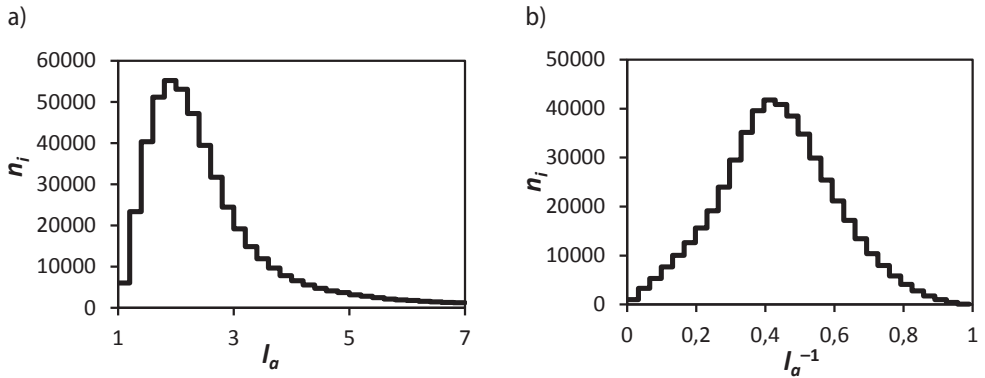


Fig. 8. Distribution of apparent interlamellar spacing l_a (a) and the reciprocal of apparent interlamellar spacing l_a^{-1} (b) with the assigned Rayleigh distribution of true interlamellar spacing l_t obtained as a result of the simulation

5. Discussion of results

The correctness of the performed computer simulation of the previously defined geometrical model of the lamellar microstructure is proven by the very good compatibility of the obtained empirical distributions of the distance between parameters l_r and l_a and the reciprocal of distance l_r^{-1} , l_a^{-1} with the analytically obtained density functions (cases A and B).

It is worth noting the characteristic property that is exhibited by the distribution of the reciprocals of random interlamellar spacing; regardless of the form of the distribution of true interlamellar spacing $f(l_t)$, this distribution characterizes in the existence of a “plateau” upto $l_r^{-1} = l_{t\max}^{-1}$. The presence of a “plateau” has already been one of the bases for verifying the compatibility of the presented model with the microstructure of coarse pearlite [12].

Obviously, the central point of the stereological description of the lamellar microstructure is the solution of integral equations (5) and (6), which can allow for estimating the distribution of true interlamellar spacing on the basis of the empirical distribution of random or apparent interlamellar spacing. Such attempts, both in the strict and the approximated forms (by way of discretization of the continuous random variable l_t), have been and still are made [14].

The presented and further-developed simulation method can be used in the future for the examination of the effect of deviations from the lamellar morphology on the results of the estimation of the stereological parameters according to the assumed model, as well as the properties of the stereological parameter estimators of this microstructure.

Acknowledgements

The work has been implemented within framework of statutory research of AGH University of Science and Technology, contract No. 11.11.110.299 AGH.

References

- [1] Hillert M.: The formation of pearlite. In: Zakay V.F., Aaronson H.I. (eds.): Decomposition of austenite by diffusional processes. Interscience, New York 1962, 197–237
- [2] Czarski A., Ryś J.: Morphology of Pearlite. Archives of Metallurgy, 32 (1987), 453–464
- [3] Doi S.N., Kestenbach H.-J.: Determination of the pearlite nodule size in eutectoid steels. Metallography, 23 (1989), 135–146
- [4] Bramfitt B.L., Marder A.R.: A transmission-electron-microscopy study of the substructure of high-purity pearlite. Metallography, 6 (1973), 483–495
- [5] Frank F.C., Puttick K.E.: Cementite morphology in pearlite. Acta Metallurgica, 4 (1956), 206–210
- [6] Kirkaldy J.S., Sharma R.C.: Stability principles for lamellar eutectoid(IC) reactions. Acta Metallurgica, 28 (1980), 1009–1021
- [7] Czarski A., Skowronek T., Osuch W.: Influence of orientation relationship between ferrite and cementite in pearlite on stability of cementite plates. Metallurgy and Foundry Engineering, 33 (2007), 41–49
- [8] DeHoff R.T., Rhines F.N.: Quantitative Microscopy. McGraw-Hill, New York 1968
- [9] Underwood E.E.: Quantitative Stereology. Addison-Wesley, 1970
- [10] Matusiewicz P., Czarski A., Adrian H.: Estimation of materials microstructure parameters using computer program SigmaScan Pro. Metallurgy and Foundry Engineering, 33 (2007), 33–40
- [11] Ryś J., Czarski A.: Quantitative analysis of lamellar structure. Proceedings of IV Symposium on Metallography, Vysoke Tatry, Czechoslovakia, 1 (1986), 25–30
- [12] Czarski A., Ryś J.: Stereological relationships for lamellar structure. Acta Stereologica, 6 (1987), 567–572
- [13] Czarski A., Głowacz E.: Relationship between mean values of interlamellar spacings in case of lamellar microstructure like pearlite. Archives of Metallurgy and Materials, 55 (2010), 101–105
- [14] Czarski A., Ryś J.: Quantitative analysis of lamellar structure. Prace Komisji Metalurgiczno-Odlewniczej, Polska Akademia Nauk Oddział Kraków, Metalurgia, 35 (1988), 35–42
- [15] Czarski A., Matusiewicz P.: Some aspects of estimation accuracy of mean true interlamellar spacing. Metallurgy and Foundry Engineering, 38 (2012), 133–140
- [16] Wiczorkowski R., Zieliński R.: Komputerowe generatory liczb losowych. WNT, Warszawa 1997
- [17] Gentle J.E.: Random Number Generation and Monte Carlo Methods (Statistics and Computing). Springer, 2004
- [18] Devore J.L.: Probability and Statistics for Engineering and the Sciences. 7th Edition, Brooks/Cole, 2009
- [19] Forbes C., Evans M., Hastings N., Peacock B.: Statistical Distributions. 4th Edition, Wiley, 2011